Journal of Signal Processing, Vol.23, No.4, pp.197-200, July 2019

SELECTED PAPER AT NCSP'19

Jumping Movement of Biped Robot Using Closed Link Legs and Spring Mechanism

Yu Yamanaka, Hiroshi Suzuki and Takashi Yasuno

Graduate School of Advanced Technology and Science, Tokushima University
2-1 Minami-Josanjima, Tokushima 770-8506, Japan
E-mail: yamanaka-y@ee.tokushima-u.ac.jp
{suzuki.hiroshi,yasuno.takashi}@tokushima-u.ac.jp

Abstract

We describe the mechanism and attitude control of a biped robot using a spring-damper mechanism for jumping movement. To improve the movement performances of the biped robot, it is necessary to incorporate the leap period into movements such as jumping, which is also expected to further improve surmountability on irregular terrain. To obtain the instantaneous power required for jumping, the proposed robot has a spring damper on its legs. We also designed an attitude controller that stabilizes the attitude of the robot after landing from the jumping movement. The usefulness of the designed controller is demonstrated by physical simulations.

1. Introduction

In the movement mechanism of a robot, a biped-type mechanism has superior adaptability to rough and discontinuous terrain. Therefore, research on biped robots that overcome various types of terrain is actively conducted [1][2]. However, a legged robot has the disadvantages of lower movement velocity than a wheel robot on a flat field and difficulty of control owing to the instability of attitude. These are obstacles to the practical application of biped robots. To improve the movement velocity of a biped robot, it is necessary to incorporate the leap period into its movement, but this is difficult to realize using only the output force of the motor. On the other hand, many animals have a spring damper mechanism consisting of muscles and tendons, that enables them to obtain the instantaneous power required for running and jumping.

In this paper, we propose a leg mechanism using a spring damper, and design a controller to stabilize the attitude of the robot after landing from jumping movement. The robot model consists of an upper body and four rigid links and joints making up the legs. The attitude controller of the robot is designed as an integral-type optimum servo using the linear quadratic regulator (LQR) method [3]. The LQR method can be applied to multiple input multiple output (MIMO) system, and can yield a design of the controller as a servo system for attitude control on the ground. Simulation results of vertical jumping indicate the usefulness of the spring damper in jumping motion. The effectiveness of the designed controller is confirmed from the simulation results of attitude control after landing from a jumping movement.

2. Robot Model

Figure 1 shows a simple rigid body model of the proposed biped robot. This model has a spring damper mechanism at the center of its legs to obtain the instantaneous power required for jumping. The proposed leg has a closed link mechanism composed of four equal-length rigid links, and the spring damper is inserted in a vertical diagonal line of the closed link as an elastic element. Also, the hip and ankle joints are driven for attitude control and the hip joint is also driven for jumping. The spring stiffness and natural length are set such that gravity and the spring force are balanced at the knee joint angle θ_k of 90 degrees. The limitations of the hip joint angle θ_h and ankle joint angle θ_a shown in Fig. 1(a) are from 5 to 80 degrees. The sizes and weights of the robot model are set as shown in Table 1, and the parameters of the spring damper are set as shown in Table 2.

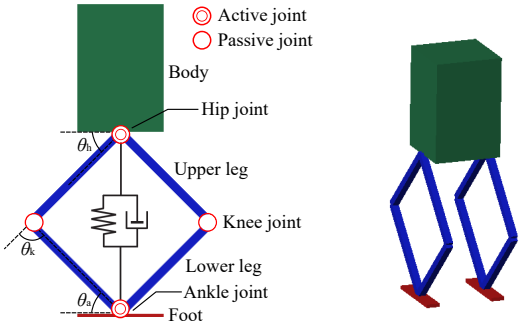

(a) 2D view (b) 3D view

Figure 1: Robot model

3. Controller Design

Table 1: Size and weight of robot

Element	Size [cm]	Weight [kg]
Body	$10 \times 10 \times 15$	1
Upper leg	$1 \times 1 \times 15$	0.2
Lower leg	$1 \times 1 \times 15$	0.2
Foot	$10 \times 2 \times 0.5$	0.3

Table 2: Spring-damper parameters

Spring stiffness	446 N/m
Damping coefficient	2 N·s/m
Natural length	23.2 cm

3.1 Mathematical model of robot

To design the integral-type optimum servo, the linear state equation of the system is required. To consider the attitude control in the sagittal plane of the robot model, as shown in Fig. 1, we assumed a 2-link manipulator as the robot model. Therefore, we can design the controller using the state equation of the 2-link manipulator model. Although the apparent length of the robot leg varies depending on the knee joint angle θ_{k}, we formulated the model assuming the knee joint angle θ_{k} to be fixed at 90 degrees. The robot model can be represented as in Figs. 2 and 3. The robot model is formulated under the assumption that the foot of the robot is grounded and it does not slip. For the 2-link manipulator model shown in Fig. 2, the state variable $\boldsymbol{x}$ is $[q_1\ \dot{q}_1\ q_2\ \dot{q}_2]^T$ and the input $\boldsymbol{u}$ is $[\tau_1\ \tau_2]^T$. q_1 is the angle of the first link from the vertical, and q_2 is the relative angle of the second link from the first link. The state equation is linearized at the origin of the model as Eq. (1), where τ_1 and τ_2 are input torques for the first and second joints, respectively.

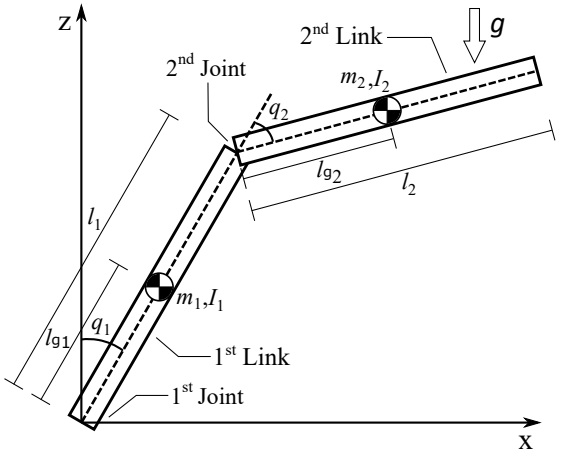

Figure 2: Two-link manipulator model

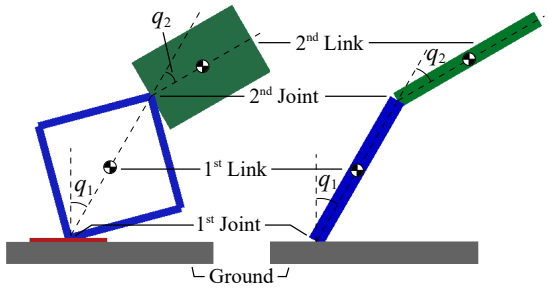

Figure 3: Model replacement

$$\dot{\boldsymbol{x}} = \boldsymbol{A}_{\mathrm{r}}\boldsymbol{x} + \boldsymbol{B}_{\mathrm{r}}\boldsymbol{u} \tag{1}$$

where

$$\boldsymbol{A}_{\mathrm{r}} = \begin{bmatrix} 0 & 1 & 0 & 0 \\ \alpha_1/\gamma & 0 & \alpha_2/\gamma & 0 \\ 0 & 0 & 0 & 1 \\ \alpha_3/\gamma & 0 & \alpha_4/\gamma & 0 \end{bmatrix},\ \boldsymbol{B}_{\mathrm{r}} = \frac{1}{\gamma}\begin{bmatrix} 0 & 0 \\ \beta_1 & \beta_2 \\ 0 & 0 \\ \beta_3 & \beta_4 \end{bmatrix}$$

$$\alpha_1 = (m_1 m_2 l_{\mathrm{g}1} l_{\mathrm{g}2}^2 + m_2 l_1 I_2 + m_1 l_{\mathrm{g}1} I_2)g$$

$$\alpha_2 = -m_2^2 l_1 l_{\mathrm{g}2}^2 g$$

$$\alpha_3 = (m_1 m_2 l_{\mathrm{g}1}^2 l_{\mathrm{g}2} - m_1 m_2 l_{\mathrm{g}1} l_{\mathrm{g}2}^2 - m_1 m_2 l_1 l_{\mathrm{g}1} l_{\mathrm{g}2} - m_1 l_{\mathrm{g}1} I_2 g + m_2 l_{\mathrm{g}2} I_1 - m_2 l_1 I_2)g$$

$$\alpha_4 = (m_2^2 l_1^2 l_{\mathrm{g}2} + m_2^2 l_1 l_{\mathrm{g}2}^2 + m_1 m_2 l_{\mathrm{g}1}^2 l_{\mathrm{g}2} + m_2 l_{\mathrm{g}2} I_1)g$$

$$\beta_1 = m_2 l_{\mathrm{g}2}^2 + I_2,\ \beta_2 = \beta_3 = -(m_2 l_{\mathrm{g}2}^2 + m_2 l_1 l_{\mathrm{g}2} + I_2)$$

$$\beta_4 = m_2 l_1^2 + 2 m_2 l_1 l_{\mathrm{g}2} + m_1 l_{\mathrm{g}1}^2 + m_2 l_{\mathrm{g}2}^2 + I_1 + I_2$$

$$\gamma = m_2 l_1^2 I_2 + m_1 m_2 l_{\mathrm{g}1}^2 l_{\mathrm{g}2}^2 + m_1 l_{\mathrm{g}1}^2 I_2 + m_2 l_{\mathrm{g}2}^2 I_1 + I_1 I_2$$

3.2 Integral-type optimum servo

In general, a linear system is represented by a state equation as

$$\dot{\boldsymbol{x}} = \boldsymbol{A}\boldsymbol{x} + \boldsymbol{B}\boldsymbol{u} \tag{2}$$

The controller of the system may be designed on the basis of the LQR method, which is an optimization method, with the control input $\boldsymbol{u}$ that minimizes the evaluation function J as follows

$$\begin{aligned} &\text{Minimize} \quad J = \int_0^\infty (\boldsymbol{x}^T \boldsymbol{Q}\boldsymbol{x} + \boldsymbol{u}^T \boldsymbol{R}\boldsymbol{u})dt \\ &\text{Subject to} \quad \dot{\boldsymbol{x}} = \boldsymbol{A}\boldsymbol{x} + \boldsymbol{B}\boldsymbol{u} \end{aligned} \tag{3}$$

where $\boldsymbol{x} \in \mathbb{R}^n$ is the state of the system, $\boldsymbol{u} \in \mathbb{R}^m$ is the input of the system, $\boldsymbol{Q} \in \mathbb{R}^{n \times n}$ is the state weight matrix, and $\boldsymbol{R} \in \mathbb{R}^{m \times m}$ is the input weight matrix. In the integral-type optimum servo, the deviation system and the state deviation integral value are used for the evaluation function as

$$J_{\mathrm{s}} = \int_0^\infty (\tilde{\boldsymbol{x}}^T \boldsymbol{Q}_1 \tilde{\boldsymbol{x}} + \tilde{\boldsymbol{w}}^T \boldsymbol{Q}_2 \tilde{\boldsymbol{w}} + \tilde{\boldsymbol{u}}^T \boldsymbol{R}\tilde{\boldsymbol{u}})dt \tag{4}$$

where $\tilde{\boldsymbol{x}} \in \mathbb{R}^n, \tilde{\boldsymbol{w}} \in \mathbb{R}^m$ and $\tilde{\boldsymbol{u}} \in \mathbb{R}^m$ are the state, integral values and input deviations, and $\boldsymbol{Q}_1 \in \mathbb{R}^{n\times n}$ and $\boldsymbol{Q}_2 \in \mathbb{R}^{m\times m}$ are weight matrixes of the state and integral values, respectively. The output equation of the system is

$$\boldsymbol{y} = \boldsymbol{C}\boldsymbol{x} \tag{5}$$

when the Riccati equation is set such that

$$\begin{bmatrix} \boldsymbol{A}^T & -\boldsymbol{C}^T \\ \boldsymbol{O} & \boldsymbol{O} \end{bmatrix} \boldsymbol{P} + \boldsymbol{P} \begin{bmatrix} \boldsymbol{A} & \boldsymbol{O} \\ -\boldsymbol{C} & \boldsymbol{O} \end{bmatrix} - \boldsymbol{P} \begin{bmatrix} \boldsymbol{B} \\ \boldsymbol{O} \end{bmatrix} \boldsymbol{R}^{-1} \begin{bmatrix} \boldsymbol{B}^T & \boldsymbol{O} \end{bmatrix} \boldsymbol{P} + \begin{bmatrix} \boldsymbol{Q}_1 & \boldsymbol{O} \\ \boldsymbol{O} & \boldsymbol{Q}_2 \end{bmatrix} = \boldsymbol{O} \tag{6}$$

Using the solution $\boldsymbol{P}$ of Eq. (6), the state feedback gain $\boldsymbol{F}$, the integral feedback gain $\boldsymbol{G}$, and the reference input feedback gain $\boldsymbol{H}$ can be obtained as

$$\boldsymbol{F} = -\boldsymbol{R}^{-1}\boldsymbol{B}^T\boldsymbol{P}_{11} \tag{7}$$

$$\boldsymbol{G} = -\boldsymbol{R}^{-1}\boldsymbol{B}^T\boldsymbol{P}_{12} \tag{8}$$

$$\boldsymbol{H} = \begin{bmatrix} -\boldsymbol{F} + \boldsymbol{G}\boldsymbol{P}_{22}^{-1}\boldsymbol{P}_{12}^T & \boldsymbol{I} \end{bmatrix} \begin{bmatrix} \boldsymbol{A} & \boldsymbol{B} \\ \boldsymbol{C} & \boldsymbol{O} \end{bmatrix}^{-1} \begin{bmatrix} \boldsymbol{O} \\ \boldsymbol{I} \end{bmatrix} \tag{9}$$

Using each feedback gain, the optimal control input $\boldsymbol{u}_{\mathrm{opt}}$ is obtained as

$$\boldsymbol{u}_{\mathrm{opt}} = \boldsymbol{F}\boldsymbol{x} + \boldsymbol{G}\boldsymbol{w} + \boldsymbol{H}\boldsymbol{r} - \boldsymbol{G}\boldsymbol{P}_{22}^{-1}\boldsymbol{P}_{12}^T\boldsymbol{x}_0 - \boldsymbol{G}\boldsymbol{w}_0 \tag{10}$$

where $\boldsymbol{r}$ is the reference input and $\boldsymbol{x}_0$ and $\boldsymbol{w}_0$ are the state and deviation integral values at the time when the reference input changes, respectively. For our developed model, the weight matrixes are set as

$$\boldsymbol{Q}_1 = \mathrm{diag}(50,\ 0,\ 250,\ 0)$$
$$\boldsymbol{Q}_2 = \mathrm{diag}(35,\ 25)$$
$$\boldsymbol{R} = \mathrm{diag}(1,\ 1)$$

4. Simulation Results

The effectiveness of the controller is evaluated from simulation results. For the simulation environment, Simscape Multibody in MATLAB/Simulink is used. Simscape Multibody is a useful modeling and physical simulation environment for a multi-rigid-body mechanical system.

4.1 Contribution of spring damper to jumping motion

The jumping motion is examined to investigate the characteristics of the proposed robot model. Sinusoidal torque with a constant frequency is input to the hip joint. The hip joint torque is given in the direction that opens and closes the crotch. The amplitude of the sinusoidal torque is set to 3 Nm and the frequency is set to 2.35 Hz. Here, the frequency suitable for a high jump was determined by trial and error. The simulation result is shown in Fig. 4 and indicates that the robot succeeds in hopping. If the same torque is input to the robot without the spring damper mechanism, the robot cannot jump. Therefore, it is confirmed that the application of the spring damper mechanism makes hopping possible. From the result, we found that the spring damper force is saturated at about -30 N owing to the limitation of the joint angle. Therefore, the spring stiffness can be optimized in consideration of leg size for effective hopping.

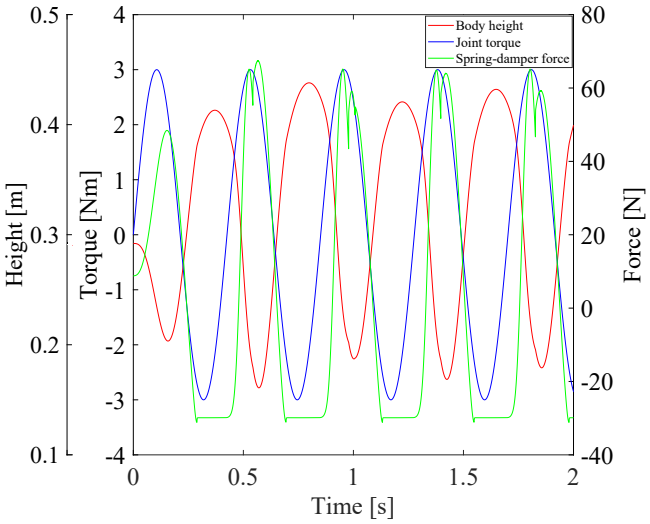

Figure 4: Simulation results for jumping motion

4.2 Attitude stabilization on the ground

The control performance of the designed attitude controller is confirmed from the static simulation for the upright state. The control objective is to converge the attitude angles of the robot q_1 and q_2, to zero from the initial angles. The initial values of angles q_1 and q_2 are set to 10 degrees. The control result of q_1 and q_2 is shown in Fig. 5. We can confirm that the control to converge q_1 and q_2 to an upright state is possible.

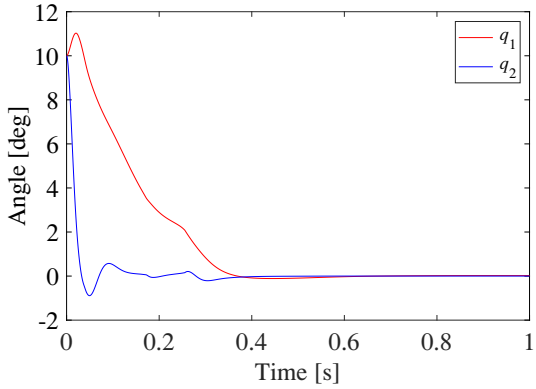

Figure 5: Simulation results for attitude stabilization

4.3 Jumping movement and attitude stabilization after landing

A simulation of jumping movement is performed to confirm the stability of the attitude after landing. The robot jumps upon inputting a constant torque of 3 Nm to the hip joint in the direction that closes the crotch. This torque is input until the first takeoff of the foot. The initial states are set to $q_1 = 5, q_2 = 0$, and $\theta_k = 150$ degrees. In the air, the foot angle is controlled by the PD controller so that the foot becomes horizontal, and the hip joint torque is set to zero. When the foot comes in contact with the ground, the attitude is stabilized using the designed controller. Figure 6 shows the simulation results for level ground, and Figs. 7(a) and 7(b) show the attitude angles, joint torques, and spring damper force. As seen in Fig. 6, the robot jumped and the attitude stabilized after landing. Also, the robot moved about 17 cm in the horizontal direction. The robot corrects the attitude toward the upright state at each landing, and it was possible to stabilize q_1 and q_2 to zero after landing. In Fig. 7, the force of the spring is larger than the gravity force acting on the robot of about 30 N, and it assists in jumping. Figure 6 shows that the ankle joint outputs a large torque at first landing at 0.5 s, and it works to cancel the horizontal kinetic momentum. Therefore there is a possibility that the required torque can be reduced by adjusting the weight matrixes or attitude control in the air. q_2 increases at around 0.8 s, which is thought to be because the robot jumps owing to the effect of the spring after landing, and attitude control in the air is not performed. The robot bounces backward owing to the effect of the spring after landing but this is undesirable for stability. To prevent the robot from bouncing backward, control to suppress the vibration of the spring after landing is also necessary.

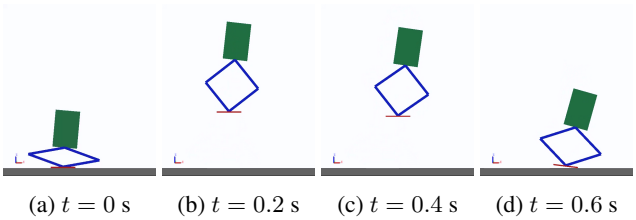

(a) $t = 0$ s (b) $t = 0.2$ s (c) $t = 0.4$ s (d) $t = 0.6$ s

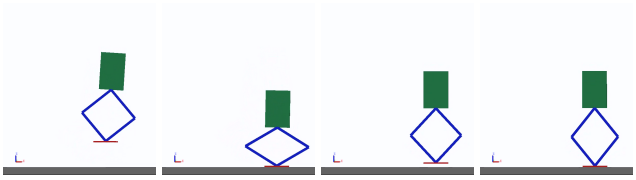

(e) $t = 0.8$ s (f) $t = 1.0$ s (g) $t = 1.2$ s (h) $t = 1.4$ s

Figure 6: State of jumping and landing

5. Conclusions

In this paper, we proposed a biped robot in which a spring damper mechanism is used to realize jumping movement and we designed an attitude controller. From the simulation results, we confirmed that the robot can jump using the proposed spring damper mechanism and can stabilize its attitude after landing using the proposed attitude controller. However, the current attitude controller only controls the attitude on the ground. Therefore, attitude control in the air is required to achieve efficient jumping movement. Designing an in-air attitude controller and improving jumping movement are future tasks. In addition, it is necessary to adjust the parameters of the controller in consideration of modeling errors before the controller can be applied to a real robot.

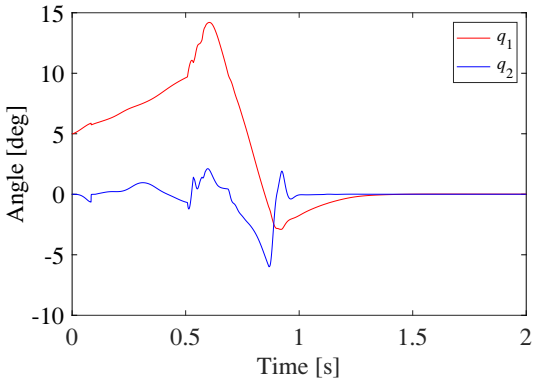

(a) Attitude angles

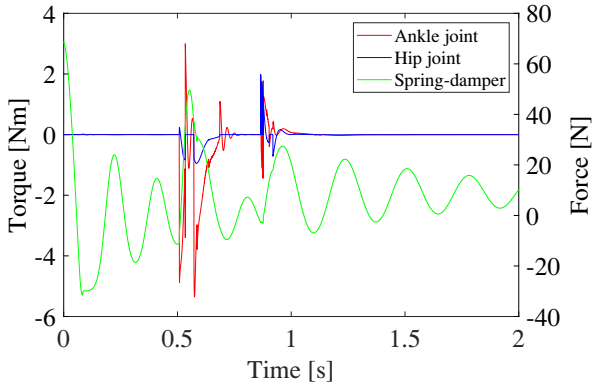

(b) Joint torques and spring-damper force

Figure 7: Simulation results

References

[1] S. Kuindersma, R. Deits, M. Fallon, A. Valenzuela, H. Dai, F. Permenter, T. Koolen, P. Marion and R. Tedrake: Optimization-based locomotion planning, estimation, and control design for the atlas humanoid robot, Autonomous Robots, Vol. 40, pp. 429-455, 2016.

[2] T. Apgar, P. Clary, K. Green, A. Fern and J. Hurst: Fast online trajectory optimization for the bipedal robot Cassie, Robotics: Science and Systems 2018.

[3] M. Ikeda and N. Suda: Synthesis of optimal servosystems, Transactions of the Society of Instrument and Control Engineers, Vol. 24, No. 1, pp. 40-46, 1988.